

Facile Fabrication of Screen-Printed Carbon Electrodes for Electrochemical Sensors

P. Sarmphim^{1*}, K. Teeparukpun¹, S. Wunsri¹, S. Sorngodchakon¹,
W. Duangsiri¹, P. Tapparak¹ and C. Sirisathitkul²

¹Department of General Education, Faculty of Liberal Arts,
Rajamangala University of Technology Srivijaya, Songkhla, Thailand

²Division of Physics, School of Science,
Walailak University, Nakhon Si Thammarat, Thailand

Received 4 August 2020, Revised 11 December 2020, Accepted 15 February 2021

ABSTRACT

Carbon pastes were applied in fabricating screen-printed carbon electrodes (SPCEs) for versatile electrochemical analyses. The electrochemical behavior of the homemade system, consisting of a working electrode, a counter electrode and a reference electrode, was investigated by the cyclic voltammetry (CV) of ferricyanide at a low concentration. The homemade SPCEs gave standard CV characteristics with sensitive electrochemical behaviors. Due to the surface roughness, the cathodic and anodic current peaks (I_{pc} and I_{pa}) of the homemade SPCEs were significantly higher than those of commercial DropSens 110 SPCEs at a 90 % confidence level (P value 0.1). However, the reproducibility of homemade SPCEs ($n=3$) by manual pasting was lower than commercial DropSens 110. The novelty in making electrodes on a polyester substrate by using carbon pastes substantially reduces the production cost. The materials and process used for these homemade SPCEs showed the potential for a variety of electrochemical sensors.

Keywords: Screen-printed electrode, carbon paste, cyclic voltammetry, potentiostat, electrochemical sensor

1. INTRODUCTION

Bulky electrochemical electrodes and beaker-type cells have been very useful in electro-analytical chemistry but lag behind in many features such as cost, portability, usability and on-site analysis. Screen printing on planar substrates by forcing suitable inks through a patterned stencil or mask is an adaptive technique to overcome these disadvantages. The resulting screen-printed electrodes (SPEs) have already been implemented in many real-life applications [1-3]. This is fueled by a billion-dollar per year market of the glucose sensing. The incorporation of SPEs enables individuals to measure their blood glucose levels at home [4]. In addition to commercially available electrochemical glucose sensors, these SPEs have been regularly utilized for other biomedical applications including determinations of fructose in beverages [5] glucose in fermentation processes[2], as well as diagnosis of infectious disease and virus [6, 7]. The potential use of SPEs in corona virus detections has also been suggested [8, 9].

The use of carbon in screen printing of electrodes has an important part in the commercial success of glucose biosensors [10] and several other detections including dopamine [11] and heavy metals in environments [12]. The carbonaceous nanomaterials possess unique characteristics of high electrical conductivity and chemical stability with large active surface areas. Their reproducibility and low-cost are attractive for the mass production [13]. Screen-printed carbon electrodes (SPCEs) are therefore highly promising for versatile electrochemical sensors [14].

*E-mail of corresponding author: pharunee.t@rmutsv.ac.th

SPEs are conventionally produced by using printing machines. Most commercial SPEs with excellent performance are mainly distributed at high prices. Literature research suggested that DropSens electrodes from Metrohm corporation set a standard for electrochemical sensors [15, 16]. The 'DropSens 110' electrodes have mostly been implemented in biosensors for detecting neurotransmitter dopamine [11] and monitoring glucose concentration [2].

It is still a challenge to develop a facile fabrication process for low-cost SPCEs. The novelty of this work is to apply carbon pastes in SPCEs for versatile electrochemical analyses. The homemade SPCE is designed to resemble commercial electrodes with suitable cable connections with a potentiostat. The performance of this homemade electrode is compared to that of the DropSens 110.

2. THEORY

This work involves the reduction and oxidation of ferri/ferrocyanide ($\text{Fe}(\text{CN})_6^{3-}/\text{Fe}(\text{CN})_6^{4-}$) on the working electrode surface, referred to as a redox couple reaction. A typical cyclic voltammogram is presented in Figure 1 [5]. When the potential is scanned negatively (cathodically) from point a to c, $\text{Fe}(\text{CN})_6^{3-}$ is steadily decreased near the electrode as it is reduced to $\text{Fe}(\text{CN})_6^{4-}$ according to the process in Eq. (1). The corresponding current is referred to as the cathodic current. After the peak cathodic current (I_{pc}) is obtained at point b, the current is decreased by the delivery of additional $\text{Fe}(\text{CN})_6^{3-}$ via the diffusion from the bulk solution. The volume of solution at surface of the electrode containing the $\text{Fe}(\text{CN})_6^{4-}$, called the diffusion layer, continue to grow throughout the scan. This slows down the mass transport of $\text{Fe}(\text{CN})_6^{3-}$ to the electrode. Upon scanning to more negative potentials, the rate of diffusion of $\text{Fe}(\text{CN})_6^{3-}$ from the bulk solution to the electrode surface therefore become slower, resulting in a decrease in the current in the continuous scan. When the scan direction is reversed and the potential is scanned in the positive (anode) direction (from point c to e), the $\text{Fe}(\text{CN})_6^{4-}$ from reduction at the electrode surface is oxidized back to $\text{Fe}(\text{CN})_6^{3-}$ as the applied potential become more positive with process in Eq. (2). After the anodic current reaches the peak (I_{pa}) at point d, the current is decreased by the diffusion mechanism.

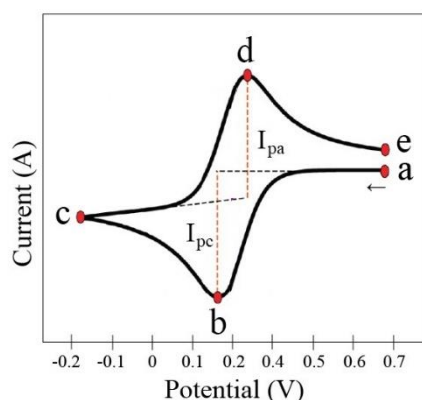
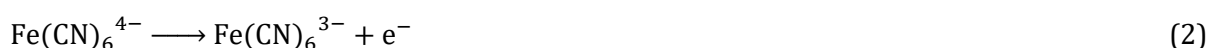
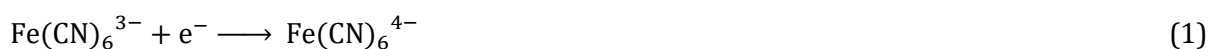


Figure 1. Typical cyclic voltammogram of a redox couple reaction.

The electron transfer rates from the reversible, quasi-reversible and irreversible electrochemical reactions are different. The best performance of electrodes corresponding to the reversible electrochemical reactions is limited. The electron kinetics are much faster than the rate of mass transport according to the Nernst equation. The applied potential (E) is related to the potential of species or analyte (E^0) and the concentration of oxidized [Ox] and reduced [Red] analyte in the system at equilibrium as shown in Eq. (3).

$$E = E^0 + \frac{RT}{nF} \ln \frac{[Ox]}{[Red]} = E^0 + 2.30226 \frac{RT}{nF} \log \frac{[Ox]}{[Red]} \quad (3)$$

where F is Faraday's constant and R is the universal gas constant, n is the number of electrons and T is the temperature. By applying the Nernst equation to the one-electron reduction of $\text{Fe}(\text{CN})_6^{3-}$ to $\text{Fe}(\text{CN})_6^{4-}$, n is set at 1 and the activities are replaced with their concentrations which are more experimentally accessible. Eq. (4) is obtained as follows.

$$E = E^0 + 2.3026 \frac{RT}{F} \log \frac{[\text{Fe}(\text{CN})_6^{4-}]}{[\text{Fe}(\text{CN})_6^{3-}]} \quad (4)$$

In the case of electrochemically reversible process with rapid electron transfers, the peak-to-peak separation $\Delta E_p = (E_p^{\text{ox}} - E_p^{\text{red}})$ is relatively small at the reversible limit, where $\Delta E_p = 2.22 RT/nF$ corresponding to a value of 57 mV at 298 K with $n = 1$ [17].

3. MATERIAL AND METHODS

3.1 Materials, reagents and apparatus

The carbon graphite paste (C2130925D1) and silver/silver-chloride (Ag/AgCl) paste (C2090225P7) were obtained from Gwent Electronic Materials. Potassium ferricyanide ($\text{K}_3\text{Fe}(\text{CN})_6$) and potassium chloride (KCl) were purchased from Sigma-Aldrich (UK) whereas a 0.35 mm-thick polyester sheet was obtained from an online supplier. Deionized (DI) water was supplied by Central Equipment Division, Faculty of Science, Prince of Songkla University. Commercial DropSens 110 SPCEs, obtained from Metrohm corporation, were used as a comparison. The electrochemical data was collected by the 910 PSTAT mini potentiostat (Metrohm Autolab), controlled by PSTAT software 1.1. The SPCEs were connected to the potentiostat via electrode cables.

3.2 Fabrication and morphological characterization of the homemade SPCEs

To fabricate SPCEs for this work, the mask was designed using Illustrator CC 2019. The mask was printed on a sticky paper and cut through the designed shape with the cutting machine. The mask was then placed on a 10 mm \times 30 mm piece of polyester schematically shown in Figure 2. Electrodes were manually pasted by the following steps. Firstly, the Ag/AgCl ink was applied on the reference electrode track by using a small brush and then dried for 15 min. The carbon ink was then applied in the counter and working electrodes as well as all conductive tracks before drying in an oven at 60 °C for 30 min. After the curing step, the mask was removed, a protective layer was applied by using sticky tape to insulate the conductive tracks from the three electrodes. Finally, the electrodes were rinsed with DI water and then dried at room temperature. The

fabricated SPCEs were kept in desiccator until their use and characterization. The surfaces of commercial and homemade electrodes were compared by Scanning Electron Microscopy (SEM; Quanta 400 FEI). The surface topographies were also record using Atomic Force Microscopy (AFM; Nanosurf AG., FlexAFM). In addition to the imaging, the root-mean-square roughness (S_q) of both electrodes were determined by examining a $100\ \mu\text{m} \times 100\ \mu\text{m}$ area of electrodes by AFM.

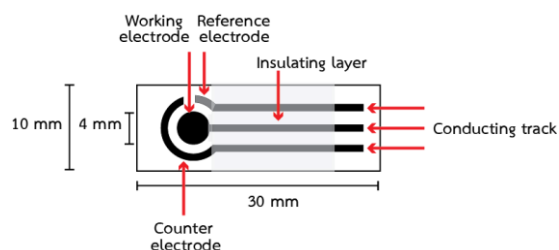


Figure 2. Schematic representation the homemade SPCEs.

3.3 Electrochemical measurement

A schematic drawing of the electrochemical system is shown in Figure 3. SPCEs were connected to the potentiostat via an electrode connector and a potentiostat was connected to the computer via a USB cable.

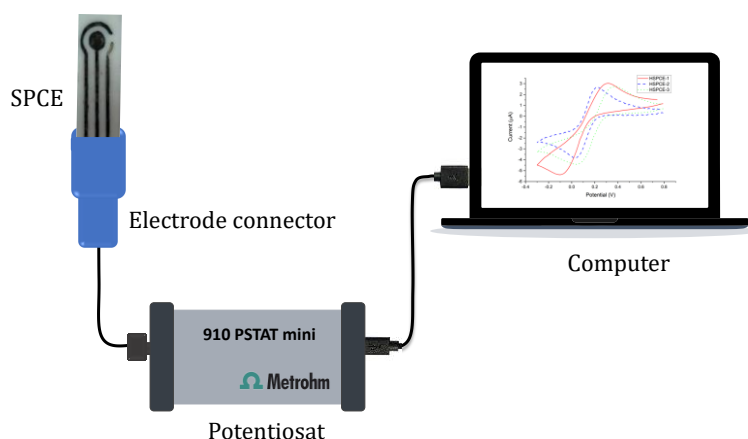


Figure 3. A three-electrode system connecting a computer-controlled potentiostat for CV experiments.

The cyclic voltammetry (CV) was performed by depositing a $200\ \mu\text{l}$ of $0.5\ \text{mM}$ ferricyanide, in $0.1\ \text{M}$ phosphate buffer pH 7.5 containing $0.1\ \text{M}$ potassium chloride, onto the surface of the SPCEs. The scan rate was $10\ \text{mVs}^{-1}$. The initial and final potentials were $+0.8\ \text{V}$ whereas the switching potential was $-0.3\ \text{V}$. The potential was held at $+0.8\ \text{V}$ for $10\ \text{s}$ before the initial cycle. To obtain reproduced electrochemical signal, the surface pre-treatment of electrodes was carried out by applying several CV cycles on an electrochemical assay until the CV characteristic was steady. Then, the cyclic voltammogram was recorded and used to calculate peak current intensity, peak potentials of the anodic and cathodic processes as well as peak-to-peak separation. The reproducibility of the homemade SPCEs was investigated by repeated measurements on three samples, referred to as HSPCE-1, HSPCE-2 and HSPCE-3. A similar experiment was performed using commercial DropSens 110 for a comparative study of electrode performance.

4. RESULTS AND DISCUSSION

4.1 Morphology of SPCEs

The commercial DropSens 110 and homemade SPCEs are shown in Figure 4. Both types of electrode are composed of a 4 mm diameter carbon working electrode, a carbon counter electrode and a Ag/AgCl reference electrode with carbon conducting parts as well as a layer to insulate electrodes.



Figure 4. Photograph comparing DropSens 110 and HSPCE.

Figure 5 shows the top view SEM images of HSPCE and DropSens 110. As illustrated in Figure 5(a), the HSPCE exhibits rough surface and non-uniform morphology. Its surface is covered by small carbonaceous particles and large holes are observed in the highly magnified inset. By contrast, the DropSens 110 shows a relatively smooth surface in Figure 5(b) with rough patches exemplified in the inset.

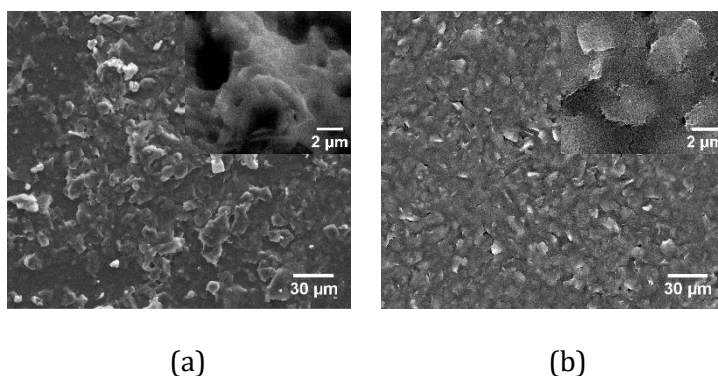


Figure 5 Top view micrographs of (a) HSPCE and (b) DropSens 110 taken by SEM.

Figures 6(a) and 6 (b) respectively show a three-dimension AFM images of HSPCE and DropSens 110. The AFM characterization agree with SEM results that the surface of HSPCE is rougher than DropSens 110 surface. From five areas selected to evaluate the surface roughness, the average S_q of HSPCE and DropSens 110 are 1457 ± 148 and 612 ± 144 nm, respectively.

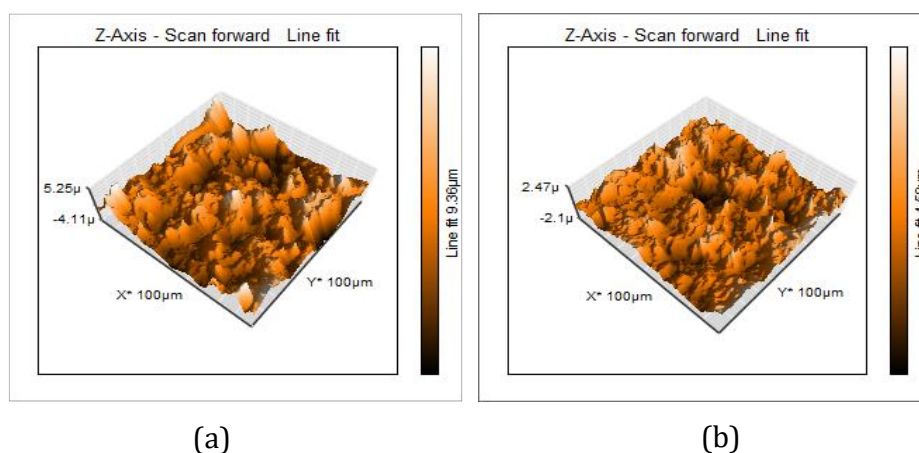


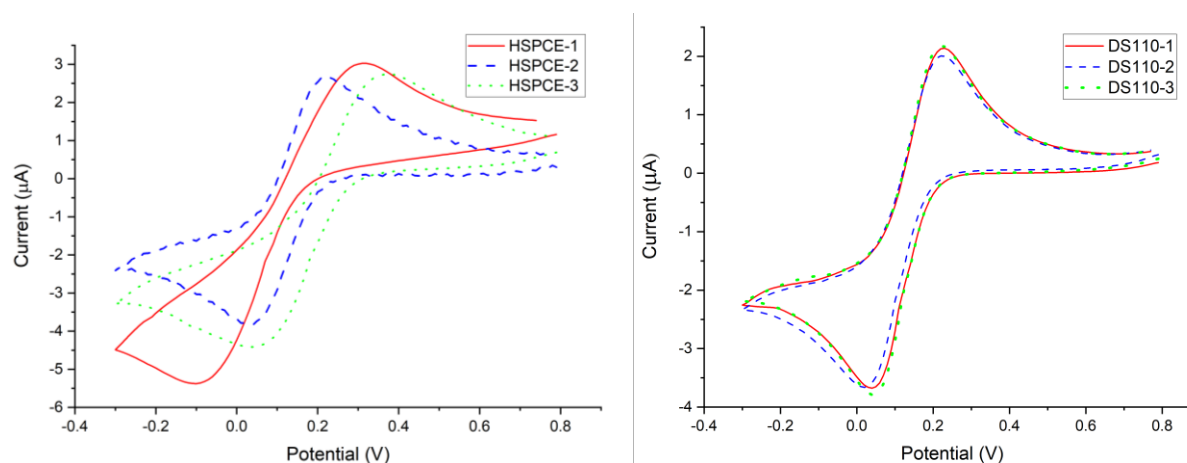
Figure 6 Three-dimensional AFM images of (a) HSCPE and (b) DropSens 110.

The manufacturing cost of the developed electrode is less than a half of imported commercial SPCEs (around 6\$ per piece). Using less silver or none at all substantially is cost-effective. In this work, the carbon ink is successfully applied to define conducting tracks and electrode areas. Ag in the reference electrode is replaced by a more stable Ag/AgCl. To prevent the reaction with an analyte, the conductive tracks are insulated by sticky tape. Additionally, the substrate material is replaced by polyester with a lower cost. The fabrication of homemade SPCEs in this work took about 45 min and several electrodes can be manufactured at the same time.

4.2 Performances of SPCEs

Initially, HSPCEs were pretreated in order to obtain repeatable electrochemical signal. From the pre-treatment, the cyclic voltammograms using HSPCE are uniform in shape, and have high peak currents. The peak to peak is lower when more CV was repeated between 10 to 30 cycles. This observation is in accordance with the previous report by Carneiro and co-workers [18].

The performance of three HSPCEs interrogated by CV was compared to three commercial SPCEs (DS110-1, DS110-2 and DS110-3) in Figure 7. The homemade SPCEs exhibit the CV characteristics comparable to DropSens 110 Commercial SPCEs. Each cyclic voltammogram was analyzed in terms of peak separation (ΔE_p), cathodic (I_{pc}) and anodic peak (I_{pa}). The mean values ($\Delta E_{p,av}$, $I_{pc,av}$ and $I_{pa,av}$) with their standard deviations are also listed in Table 1.



(a)

(b)

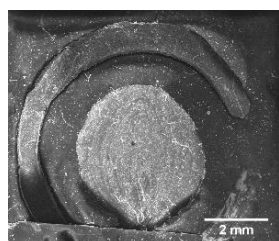
Figure 7. Cyclic voltammograms of the (a) homemade and (b) DropSens 110 SPCEs in ferri/ferrocyanide for three samples each.

In Table 1, the I_{pc} and I_{pa} of the HSPCEs are significantly higher than those of the DropSens 110 at a 90 % confidence level (P value 0.1). The average values of cathodic ($I_{pc,av}$) and anodic ($I_{pa,av}$) current peaks of HSPCEs are 4.57 ± 0.76 and 3.42 ± 0.27 μA , respectively. These current levels are comparable to those reported by Nicholas and co-workers [5]. In that work, the SPCEs were evaluated with lowly concentrated ferricyanide (0.5 mM) and used in a fructose detection [5]. The higher values of $I_{pc,av}$ and $I_{pa,av}$ of HSPCEs in Table 1 are likely due to the higher surface roughness of HSPCEs when compared to Dropsens 110. It has been reported that electrode roughness has a significant effect on the shape of cyclic voltammogram and peak currents [19]. Thus, the roughness of the HSPCEs in this work tends to improve electrochemical reactivities.

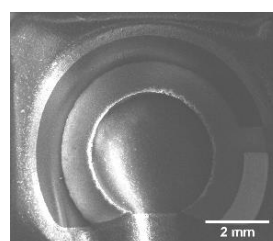
However, the HSPCEs yielded a lower electron transfer rate with a much larger standard deviation ($\Delta E_p = 300 \pm 120$ mV) than the DropSens 110. A larger variation in performance is commonly expected from homemade products. Nevertheless, the ΔE_p value as low as 170 mV from HSPCE-2 suggests that a good electron transfer rate could be obtained in SPCEs from this facile fabrication. In additions, previous works suggested that SPCEs with ΔE_p as high as 400 mV in a redox probe using $[\text{Fe}(\text{CN})_6]^{4-/3-}$ can be modified by nanoparticles to improve electron transfer rate for further applications [20, 21].

Table 1 ΔE_p , I_{pc} , I_{pa} , $\Delta E_{p,av}$, $I_{pc,av}$ and $I_{pa,av}$ using homemade and DropSens 110 SPCEs

Sample	ΔE_p (mV)	$\Delta E_{p,av}$ (mV)	I_{pc} (μA)	$I_{pc,av}$ (μA)	I_{pa} (μA)	$I_{pa,av}$ (μA)
HSPCE-1	410		5.389		3.695	
HSPCE-2	170	300 ± 120	3.874	4.57 ± 0.76	3.426	3.42 ± 0.27
HSPCE-3	330		4.46		3.149	
DS110-1	190		3.789		3.184	
DS110-2	200	190 ± 10	3.677	3.71 ± 0.07	3.109	3.11 ± 0.08
DS110-3	180		3.675		3.034	



(a)



(b)

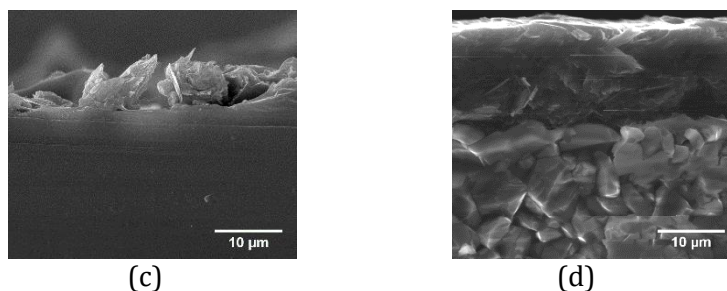


Figure 8 Top view SEM images of the working electrode of (a) HSPCE, (b) Dropsens 110, and cross-sectional view SEM images of the working electrode of (c) HSPCE and (d) Dropsens 110.

The reproducibility corresponds to a relative standard deviation of 7% or less [22, 23]. The relative standard deviations of ΔE_p , I_{pc} and I_{pa} of HSPCEs are 40, 16.6 and 7.9%, respectively, whereas those of DropSens 110 are less than 5.3%. The lack of reproducibility in HSPCEs is likely due to the non-uniform shape of working electrode as a result of the manual pasting.

The reproducibility of HSPCEs fabrication was investigated using SEM. As can be seen in Figure 8 (a), the irregular shape and thickness are observed for HSPCEs. The working electrode area was not circular. Such deviations occurred during the filling of carbon ink using a small brush. This result referred to an irregularity of weight and quantity of carbon ink in the fabrication. On the other hand, the shape of DropSens 110 shown in Figure 8 (b) is circular since this type of electrodes were fabricated with industrial machines. The cross-sections of both electrodes are also investigated. As expected, the thickness of HSPCEs in Figures 8 (c) is not uniform. On the other hand, the layer of DropSens 110 exemplified in Figures 8 (d) exhibits much regularity in shape and thickness. The lack of reproducibility of HSPCEs lead to a wide variation and shifting in reduction and oxidation peaks previously observed in Figure 7.

Nevertheless, the fabrication of SPCEs could be improved in the future work. The materials and process proposed in this worked can be incorporated into screen-printing electrochemical architectures [4]. The reproducibility can be increased by using a screen frame with holding mesh screen. In an embedded ensemble stencils design, the movements of the printing media or paste towards the substrate are constant with a flexible and resilient squeegee [24].

5. CONCLUSIONS

In this work, the SPCEs in a three-electrode system are successfully produced and their standard CV characteristics were obtained. The carbon electrodes and conductive tracks on polyester substrates utilized inks and materials with a lower cost than commercial productions. Although the performance of three samples are significantly varied as a result of manual pasting, the current sensitivity of these homemade electrodes is better than those of commercial electrodes because of higher surface roughness. Therefore, the prototype can further be developed for a variety of applications.

ACKNOWLEDGEMENTS

This work is financially supported by Rajamangala University of Technology Srivijaya. The authors would like to thank W. Limbut of Center of Excellence for Trace Analysis and Biosensor, Prince of Songkla University for his guidance and support.

REFERENCES

- [1] G. Ozcelikay, L. Karadurmus, S. I. Kaya, N. K. Bakirhan, and S. A. Ozkan, "A review: New trends in electrode systems for sensitive drug and biomolecule analysis," *Crit. Rev. Anal. Chem.*, vol. 50, no. 3, pp. 212–225, 2020.
- [2] S. Abdullah, M. Serpelloni, and E. Sardini, "Design of multichannel potentiostat for remote and longtime monitoring of glucose concentration during yeast fermentation," *Rev. Sci. Instrum.*, vol. 91, no. 5, article no. 054104, 2020.
- [3] Y. Cui, "Electronic materials, devices, and signals in electrochemical sensors," *IEEE Trans. Electron Devices*, vol. 64, no. 6, pp. 2467–2477, 2017.
- [4] C. E. Banks, C. W. Foster, and R. O. Kadara, *Screen-Printing Electrochemical Architectures*, Springer, Cham, Switzerland, 2016.
- [5] P. Nicholas, R. Pittson, and J. P. Hart, "Development of a simple, low cost chronoamperometric assay for fructose based on a commercial graphite-nanoparticle modified screen-printed carbon electrode," *Food Chem.*, vol. 241, pp. 122–126, 2018.
- [6] G. Ruiz-Vega, K. Arias-Alpizar, E. de la Serna, L. N. Borgheti-Cardoso, E. Sulleiro, I. Molina, X. Fernández-Busquets, A. Sánchez-Montalvá, F. J. Del Campo, and E. Baldrich "Electrochemical POC device for fast malaria quantitative diagnosis in whole blood by using magnetic beads, poly-HRP and microfluidic paper electrodes," *Biosens. Bioelectron.*, vol. 150, article no. 111925, 2020.
- [7] M. Manzano, S. Viezzi, S. Mazerat, R. S. Marks, and J. Vidic, "Rapid and label-free electrochemical DNA biosensor for detecting hepatitis A virus," *Biosens. Bioelectron.*, vol. 100, pp. 89–95, 2018.
- [8] L. A. Layqah, and S. Eissa, "An electrochemical immunosensor for the corona virus associated with the Middle East respiratory syndrome using an array of gold nanoparticle-modified carbon electrodes," *Microchim. Acta*, vol. 186, article no. 224, 2019.
- [9] S. Mavrikou, G. Moschopoulou, V. Tsekouras, and S. Kintzios, "Development of a portable, ultra-rapid and ultra-sensitive cell-based biosensor for the direct detection of the SARS-CoV-2 S1 spike protein antigen," *Sensors*, vol. 20, no. 11, article no. 3121, 2020.
- [10] A. Morrin, A. J. Killard, and M. R. Smyth, "Electrochemical characterization of commercial and home-made screen-printed carbon electrodes," *Anal. Lett.*, vol. 36, no. 9, pp. 2021–2039, 2003.
- [11] S. Hannah, M. Al-Hatmi, L. Gray, and D. K. Corrigan, "Low-cost, thin-film, mass-manufacturable carbon electrodes for detection of the neurotransmitter dopamine," *Bioelectrochemistry*, vol. 133, article no. 107480, 2020.
- [12] G. Chen, "Application of carbon based material for the electrochemical detection of heavy metal ions in water environment," *Int. J. Electrochem. Sci.*, vol. 15, pp. 4252–4263, 2020.
- [13] A. Sanati, M. Jalali, K. Raeissi, F. Karimzadeh, M. Kharaziha, S. S. Mahshid, and S. Mahshid "A review on recent advancements in electrochemical biosensing using carbonaceous nanomaterials," *Microchim. Acta*, vol. 186, article no. 773, 2019.
- [14] Z. Lin, G. Wu, L. Zhao, and K. W. C. Lai, "Carbon nanomaterial-based biosensors: A review of design and applications," *IEEE Nanotechnol. Mag.*, vol. 13, no. 5, pp. 4–14, 2019.
- [15] R. O. Kadara, N. Jenkinson, and C. E. Banks, "Characterisation of commercially available electrochemical sensing platforms," *Sens. Actuat. B Chem.*, vol. 138, no. 2, pp. 556–562, 2009.
- [16] P. Fanjul-Bolado, D. Hernández-Santos, P. J. Lamas-Ardisana, A. Martín-Pernía, and A. Costa-García, "Electrochemical characterization of screen-printed and conventional carbon paste electrodes," *Electrochim. Acta*, vol. 53, no. 10, pp. 3635–3642, 2008.
- [17] N. Elgrishi, K. J. Rountree, B. D. McCarthy, E. S. Rountree, T. T. Eisenhart, and J. L. Dempsey, "A practical beginner's guide to cyclic voltammetry," *J. Chem. Educ.*, vol. 95, no. 2, pp. 197–206, 2018.

- [18] M. C. C. G. Carneiro, F. T. C. Moreira, R. A. F. Dutra, R. Fernandes, and M. G. F. Sales, "Homemade 3-carbon electrode system for electrochemical sensing: Application to microRNA detection," *Microchem. J.*, vol. 138, pp. 35–44, 2018.
- [19] D. Menshykau, I. Streeter and R. G. Compton (2008). Influence of Electrode Roughness on Cyclic Voltammetry. *J. Phys. Chem. C* 2008, 112, 14428–14438.
- [20] S. Cinti, F. Arduini, M. Carbone, L. Sansone, I. Cacciotti, D. Moscone, and G. Palleschi, "Screen-printed electrodes modified with carbon nanomaterials: A comparison among carbon black, carbon nanotubes and graphene," *Electroanalysis*, vol. 27, no. 9, pp. 2230–2238, 2015.
- [21] S. Cinti, V. Mazzaracchio, I. Cacciotti, D. Moscone, and F. Arduini, "Carbon black-modified electrodes screen-printed onto paper towel, waxed paper and parafilm M@," *Sensors*, vol. 17, no. 10, article no. 2267, 2017.
- [22] R. A. Hassan, L. Y. Heng, and L. L. Tan, "Novel DNA biosensor for direct determination of carrageenan," *Sci. Rep.*, vol. 9, article no. 6379, 2019.
- [23] R. Jirakunakorn, S. Khumngern, J. Choosang, P. Thavarungkul, P. Kanatharana, and A. Numnuam, "Uric acid enzyme biosensor based on a screen-printed electrode coated with Prussian blue and modified with chitosan-graphene composite cryogel," *Microchem. J.*, vol. 154, article no. 104624, 2020.
- [24] S. Kongkaew, P. Kanatharana, P. Thavarungkul, and W. Limbut, "Studying the preparation, electrochemical performance testing, comparison and application of a cost-effective flexible graphene working electrode," *J. Colloid Interface Sci.*, vol. 583, pp. 487–498, 2021.